Structure alteration of a sandy-clay soil by biochar amendments

Giorgio Baiamonte, Claudio De Pasquale, Valentina Marsala, Giulia Cimò, Giuseppe Alonzo, Giuseppina Crescimanno & Pellegrino Conte

Journal of Soils and Sediments

ISSN 1439-0108

J Soils Sediments
DOI 10.1007/s11368-014-0960-y

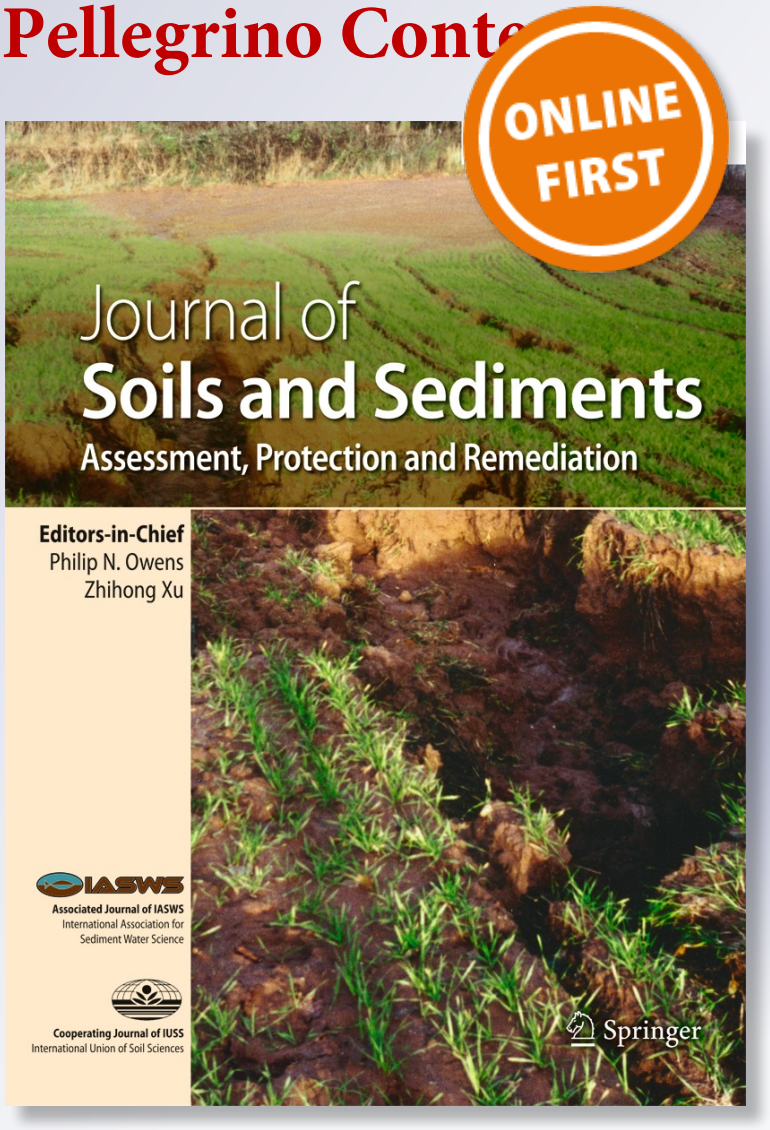

Springer

J Soils Sediments
DOI 10.1007/s11368-014-0960-y

SI: ESF EXPLORATORY WORKSHOP: NATURAL AND ANTHROPOGENIC PYROGENIC CARBON

Structure alteration of a sandy-clay soil by biochar amendments

Giorgio Baiamonte · Claudio De Pasquale · Valentina Marsala · Giulia Cimò · Giuseppe Alonzo · Giuseppina Crescimanno · Pellegrino Conte

Received: 11 April 2014 / Accepted: 2 August 2014

Abstract
Purpose The aim of the present study was to investigate structure alterations of a sandy-clay soil upon addition of different amounts of biochar (f_{bc}).
Materials and methods All the f_{bc} samples were analyzed by high energy moisture characteristic (HEMC) technique and ^{1}H nuclear magnetic resonance (NMR) relaxometry. HEMC was applied in order to evaluate aggregate stability of biochar-amended soil samples. ^{1}H NMR relaxometry experiments were conducted for the evaluation of the pore distributions through the investigation of water dynamics of the same samples.
Results and discussion The HEMC technique revealed improvement in aggregate stability through measurements of the amount of drainable pores and the stability ratio. The latter increased as the amount of biochar was raised up. The ^{1}H NMR relaxometry revealed a unimodal T_1 distribution for both the sole sandy-clay soil and the biochar. Conversely, a bimodal T_1 distribution was acquired for all the different f_{bc} samples.
Conclusions Improvement in aggregate stability was obtained as biochar was progressively added to the sandy-clay soil. A dual mechanism of water retention has been hypothesized. In particular, intra-aggregate porosity was indicated as the main responsible for molecular water diffusion when f_{bc} comprised between 0 and 0.33. Conversely, inter-aggregate porosity resulted predominant, through swelling processes, when f_{bc} overcame 0.33.

Responsible editor: Heike Knicker

G. Baiamonte · C. De Pasquale · V. Marsala · G. Cimò · G. Alonzo · G. Crescimanno · P. Conte (✉)
Dipartimento di Scienze Agrarie e Forestali, Università degli Studi di Palermo, Viale delle Scienze edificio 4, 90128 Palermo, Italy
e-mail: pellegrino.conte@unipa.it

Published online: 21 August 2014

Keywords Biochar · Biochar amended soils · High energy moisture characteristics · NMR relaxometry

1 Introduction

World's population is set to increase by 65 % (i.e. 3.7 billion people) within 2050 (Wallace 2000). Following this prediction, the additional food required to feed future generations will put further pressure on freshwater and environmental resources. According to Wallace (2000), intensive agriculture can be considered as the main responsible for freshwater loss. For this reason, about an average of 63 % of the freshwater applied to agricultural lands is forecasted to be lost through evaporation and runoff (Wallace 2000; Agnese et al. 2001, 2007). In order to prevent water wastage, soil organic amendment is suggested as a useful practice to be applied in soils stressed by intensive agricultural activities (Rawls et al. 2003).

In fact, use of organic matter appears to favour soil water retention through increase in soil porosity and in the mean pore size diameter (Rawls et al. 2003; Wagner et al. 2007; Lehmann et al. 2007; Agnese et al. 2011).

The mechanism explaining the improvement in aggregate stability by addition of organic matter has been earlier proposed by Edwards and Bremner (1967). The authors reported that soil aggregates are formed by the random combination of organo-ligands to the surface of clay particles through complexation with polyvalent cations. During this process, clay and organic particles act as a unit (rather than as separate entities) to form soil micro- (<250 μm) and macro-aggregates (>250 μm). The nature and the binding strength of the organo-mineral interactions appear to depend upon the type and surface area of the soil inorganic components. More recently, Lehmann et al. (2007) revised the aforementioned mechanism by outlining that organic matter firstly coats clay minerals, thereby forming micro-aggregates. Afterwards, the

organic matter is physically occluded into macro-aggregates by the binding of a second mineral. By this view, organic matter is sandwiched as a kind of glue between two (or more) contiguous inorganic particles. Regardless of the mechanism involved in soil aggregation, the combination of organic and inorganic systems produces a wide variety of micro-, meso- and macro-pores where water can be both physically and chemically retained together with dissolved nutrients. The latter, hence, are available for plant nutrition.

Biochar is an organic-carbon-based material obtained as by-product of the bio-energy industry (De Pasquale et al. 2012). It is a highly porous fine grained substance, whose appearance is similar to that of the coal produced by natural burning. Firstly considered as an industrial waste, in recent years, biochar became the subject of many studies because of its ability to change physical, chemical, biological and mechanical properties of soils when it is used as an amendment (Day et al. 2005; Liang et al. 2006; Sohi et al. 2010; Uchimiya et al. 2010; Yuan et al. 2011). However, it must be stated that application of biochar to soils is controversial and still a matter of debates. In fact, on the one hand, significant agronomic benefits due to char application to soils have been reported (Sohi et al. 2010; Uchimiya et al. 2010; Yuan et al. 2011). On the other hand, other studies not only reported insignificant effects of biochar on crop yields but also some adverse dose-dependent peculiarities (Kishimoto and Sugiura 1985; Mikan and Abrams 1995; Rondon et al. 2007; Rillig et al. 2010).

Alterations of hydrological characteristics following biochar amendment seem to play a very important role in the nutrient and water dynamics towards plant roots (Crescimanno and Baiamonte 1999; Lehmann et al. 2003; Karhu et al. 2011; Bagarello et al. 2013; Ouyang et al. 2013). In fact, the biochar high porous structure and large surface area can provide refuge for soil micro-organisms (e.g. mycorrhizae and bacteria) and can influence the fate of organic and inorganic nutrients (Atkinson et al. 2010). As an example, biochar additions promote crop production through the increase of nutrient availability (Chan et al. 2007; Warnock et al. 2007). Moreover, changes in soil porosity and size aggregate distribution following biochar applications that promote soil structure modifications, thereby leading also to ameliorations of many other chemical–physical soil properties such as electrical conductivity, cation exchange capacity, pH and water holding capacity (Karhu et al. 2011; De Pasquale et al. 2012; Ouyang et al. 2013).

Up to now, the effect of increasing amounts of biochar to soils have been studied mainly in relation to crop production yields, thereby leading to the conclusion that the larger the amount of added biochar, the higher is the crop yield production (Karhu et al. 2011).

The goal of the present study is the evaluation of the effects of three different biochar amounts on the aggregate stability and pore size distribution of a sandy-clay soil. Two different techniques have been applied. The high energy moisture characteristic (HEMC) technique was applied in order to investigate changes in aggregate stability through measurement of water retention curve at high matric potential (Collis-George and Figueroa 1984; Crescimanno et al. 1995; Levy and Mamedov 2002, Mamedov et al. 2010; Ouyang et al. 2013). ^{1}H NMR relaxometry with fast field cycling (FFC) setup was applied to monitor pore size distribution through the evaluation of the water dynamics in biochar/sandy-clay soil samples (Conte and Alonzo 2013). Results revealed that increasing amount of biochar added to the sandy-clay soil improved aggregate stability and increased soil porosity, thus improving the amount of water that the biochar amended soil was able to retain.

2 Materials and methods

2.1 Soil sample

The A horizon of a vertisol taken in a Sicilian farm (near Favara, Agrigento) from a vineyard field was used in this study. Soil particle analysis revealed clay, silt and sand contents of 44.8, 11.5 and 43.7 % respectively. According to these percentages, the soil was classified as sandy-clay, following the International Soil Science Society (ISSS) classification (Eswaran et al. 2002).

2.2 Biochar sample

The biochar used here was obtained from poplar (*Populus* spp. L.) wood chips which, in turn, were retrieved from dedicated short rotation forestry in the Po Valley (Gadesco Pieve Delmona, 45°10I13II N, 10°06I01II E). The age of the forestry at the cutting down was 5 years. The poplar wood chips were subjected to gasification as reported in De Pasquale et al. (2012) at a temperature of 1,200 °C. Gasification produced both syngas and biochar as by-products (De Pasquale et al. 2012). Chemical composition of the latter has been already reported in De Pasquale et al. (2012). The poplar biochar has been dried overnight in an oven set at 105 °C and then 2 mm sieved before its further use.

2.3 Sample preparation

Samples were prepared by mixing air-dried soil sample (crushed to pass a 2-mm sieve) with different amounts of biochar. Each sample was retrieved by mixing biochar (P_{bc} in g) and soil (P_s in g) according to:

$$f_{bc} = \frac{P_{bc}}{P_s + P_{bc}} \quad (1)$$

In relationship (1), f_{bc} varied as it follows: 0 (sole soil), 0.091, 0.23, 0.33 and 1.00 (sole biochar). By assuming a soil depth of 5 cm, the selected f_{bc} corresponds to 41.6, 72.2 and 84.6 t ha^{-1}, respectively, which is in line with other experimental studies (Chan et al. 2008; Spokas et al. 2009). In order to obtain the amount of biochar and soil to be mixed into a fixed sample bulk volume (V_b) corresponding to 98.2 cm^3, i.e. to a sampler (into the HEMC apparatus, see below) of 5 cm diameter and 5 cm height, Eq. (2) has been derived:

$$P_s = \frac{\rho_s \rho_{bc} \; V_b(1-f_{bc})}{\rho_s f_{bc} \; + \; \rho_{bc}(1-f_{bc})} \tag{2}$$

Here, ρ_s and ρ_{bc} are the dried soil bulk density (1.3 g cm^{-3}) and the dried biochar bulk density (0.23 g cm^{-3}), respectively.

2.4 High energy moisture characteristic (HEMC) technique

The HEMC technique is applied to investigate soil aggregate stability (Collis-George and Figueroa 1984). The technique has been chosen because of its suitability in detecting even small differences in aggregate stability (Pierson and Mulla 1989; Levy and Mamedov 2002; Mamedov et al. 2010).

The soil samples, prepared as described above, were placed in stainless steel rings (5 cm diameter, 5 cm height, 98.2 cm^3 volume) bottom capped with a porous membrane according to the procedure reported in Crescimanno et al. (1995). A relatively slow upward saturation was realized during a 45-min treatment with imposed pressure head values (h_0) of −3.5, −1.5 and 0 cm. h_0 values were referred to the top of the soil sample surfaces in the stainless steel rings. Once soil sample saturation was achieved, samples were introduced into sintered funnels. They were connected to a hanging water column whose height was manually adjusted to keep constant the difference (i.e. pressure head, h) between the position of the center of the soil sample and the water meniscus in the pipette at the end of the column (Stolte and Veerman 1991).

We measured ten different gravimetric water contents (θ, kg kg^{-1} of dried soil), corresponding to h values ranging from −6 to −150 cm. A pressure plate apparatus for determining θ values corresponding to h=−15,000 cm was also used. Table 1 reports $|h|$ and θ values obtained for all measured pressure steps. All the data in Table 1 were obtained by replicating twice the θ measurements. The gravimetric water contents for each biochar amended soil were considered significantly different according to a two-tailed t test (P=0.05).

The van Genuchten retention function given in Eq. (3) was applied to fit the experimental values (θ, $|h|$) by applying the RETC code (van Genuchten 1980; van Genuchten et al. 1991):

$$\theta \;=\; \theta_r + \frac{\theta_s - \theta_r}{(1+(\alpha|h|)^n)^m} \tag{3}$$

In Eq. (3), θ_s (kg kg^{-1}) is the saturated water content, θ_r (kg kg^{-1}) is the residual water content, α (cm^{-1}) and n are empirical parameters, and m=1−1/n (Mualem 1976). Table 2 reports the van Genutchen parameters obtained by using the RETC code. The values reported in Table 2 were used to obtain the volume of drainable pores in each sample as $\Delta\theta_g=\theta_s-\theta_r$, which represents the effective maximal saturation.

The first derivative of the van Genuchten retention curve (Eq. (4)) provides the differential water capacity curve whose maximum is centred on the pressure head value (also referred

Table 1 Experimental pairs, pressure head, $|h|$ (cm), gravimetric water content, U (g/g), obtained for the SC soil mixed with different biochar fractions

	Biochar fraction, f_{bc}				
|h| (cm)	0	0.091	0.23	0.33	1
6	0.409 a	0.690 b	1.038 c	1.441 d	2.927 e
8	0.413 a	0.690 b	1.009 c	1.431 d	2.941 e
10	0.419 a	0.691 b	1.010 c	1.421 d	2.946 e
20	0.411 a	0.670 b	0.981 c	1.355 d	2.828 e
25	0.401 a	0.645 b	0.953 c	1.301 d	2.715 e
35	0.380 a	0.603 b	0.894 c	1.232 d	2.514 e
50	0.353 a	0.557 b	0.829 c	1.144 d	2.322 e
75	0.324 a	0.508 b	0.753 c	1.053 d	2.127 e
100	0.310 a	0.474 b	0.722 c	0.989 d	2.002 e
150	0.294 a	0.447 b	0.667 c	0.857 d	1.796 e
15,000	0.157 a	0.162 a	0.217 b	0.278 c	0.321 c

For a given matric potential and a given biochar fraction values, f_{bc}, values followed by the same letter are not significantly different according to a two-tailed $t$test (P=0.05)

Table 2 Parameters of the Mualem-van Genuchten model estimated for different biochar fraction, f_{bc}

f_{bc}	θ_r (kg kg^{-1})	θ_s (kg kg^{-1})	α (cm^{-1})	n	m	SR
0	0.147	0.423	0.021	1.557	0.358	0.11
0.091	0.117	0.713	0.028	1.424	0.298	0.39
0.23	0.104	1.057	0.030	1.347	0.258	0.80
0.33	0.150	1.479	0.030	1.390	0.280	1.00
1	0.000	3.039	0.027	1.367	0.269	-

to as modal suction) associated to the most common pore size diameter:

$$\frac{d\theta}{dh} = -\alpha(\theta_s - \theta_r)(1-n)(\alpha|h|)^{n-1}(1 + (\alpha|h|)^n)^{-(1+m)} \quad (4)$$

The first derivative of Eq. (4) was set to 0 in order to obtain the modal suction ($|\tau_d|$) values according to

$$|\tau_d| = \frac{1}{\alpha}\left(\frac{n-1}{1+m\ n}\right)^{1/n} \quad (5)$$

A soil structural index (SI, kg kg^{-1} cm^{-1}) for each sample was calculated according to relation (6):

$$SI = \frac{\Delta\theta_g}{|\tau_d|} \quad (6)$$

The stability ratio (SR) was calculated as the ratio between SI obtained for the different f_{bc} and the SI value for f_{bc}=0.33. The latter is the maximum SI value obtained for the soil-biochar mixtures. For this reason, it was considered as a reference value. Although the SI value for f_{bc}=1 (sole biochar) was higher than that for f_{bc}=0.33, we did not account for it as a reference because it did not correspond to a condition of amended soil. Since SR is a dimensionless value, soil samples subjected to different treatments can be compared on a relative scale from zero to one ($0 \leq SR \leq 1$) if identical wetting rates and sample handling procedures are used for each sample (Crescimanno et al. 1995; Mamedov et al. 2010; Pierson and Mulla 1989).

2.5 NMR relaxometry investigations

Samples were taken from the HEMC apparatus at the end of each HEMC experiment at a pressure head of 150 cm. The samples were immediately analyzed by a Stelar Spinmaster Fast Field Cycling Relaxometry instrument at a constant temperature of 25 °C. The bases for the FFC NMR relaxometry have been already reported in De Pasquale et al. (2012) and Conte and Alonzo (2013). For this reason, here, we report only the experimental conditions applied for the present study. Namely, all the experiments were conducted at the fixed relaxation field (B_{RLX}) of 0.5 T. The period τ, during which B_{RLX} was applied, has been varied on 32 logarithmic spaced time sets. Sixteen scans were set with a recycle delay of 2 s. No polarization field (B_{POL}) has been applied so that all the measurements were done in non-polarized (NP) mode. A ^{1}H 90° pulse was applied at an acquisition field (B_{ACQ}) of 0.18 T in order to retrieve the free induction decay (FID) with a time domain of 100 μs and 512 points. Field switching time was 3 ms, while spectrometer dead time was 15 μs. All the recovery curves were evaluated by the UPEN algorithm (Alma Mater Studiorum, Università di Bologna, Italy) (Conte and Alonzo 2013) with the aim to obtain the longitudinal relaxation time (T_1) distributions, and therefore, information on the way water molecules are trapped in each sample (Conte et al. 2013a).

3 Results and discussion

3.1 High energy moisture characteristic (HEMC)

Soils are usually considered as a pore system continuum, characterized by two main types of pores deriving by an inter-aggregate (i.e. pore spaces between fabric units, structural pores, macro-pores) and intra-aggregate (i.e. pore spaces between particles within the fabric units, textural pores, micro-pores) soil porosity (Alaoui et al. 2011). In particular, water dynamics is mainly affected by inter-aggregate porosity in non-structured soils, whereas intra-aggregate porosity influences water movements in more structured soils (Li and Zhang 2009; Ouyang et al. 2013). The dual pore distribution depends upon the amount of organic material cementing the clay particles (Agnese et al. 2011), according to the mechanism proposed by Lehmann et al. (2007) already outlined above. According to the aforementioned behaviour, it is expected that the HEMC technique is suitable for the detection of improvement in soil aggregate stability as a consequence of biochar amendment through the measurement of water retention at high matric potential. As a matter of fact, the gravimetric water content increased with f_{bc} values at each applied pressure head (Fig. 1a). Due to the relationship between the gravimetric water content and the pore sizes (Pierson and Mulla 1989), we may infer that biochar addition to the sandy-clay soil results in the increase of the space available for water retention. Figure 1a also shows that the largest amount of gravimetric water content occurred when the sole biochar was investigated (f_{bc}=1). This indicates that the inter-aggregate porosity was more effective in the organic matter rather than in the sole soil or in the biochar-amended soil samples. Moreover, the U increment observed when f_{bc} switched from 0.33 to 1 appeared remarkably larger than those measured when f_{bc} was switched from 0 to 0.091, 0.091 to 0.23 and 0.23 to 0.33 (Fig. 1a). This behaviour can be explained by the soft nature of the organic matter which allows only system swelling as water diffuses into biochar.

The effect of biochar on pore sizes can be better evaluated by analysing Fig. 1b which reports the first derivative of the water retention curves reported in Fig. 1a. In particular, Fig. 1b shows the distribution of the matric potentials associated to the

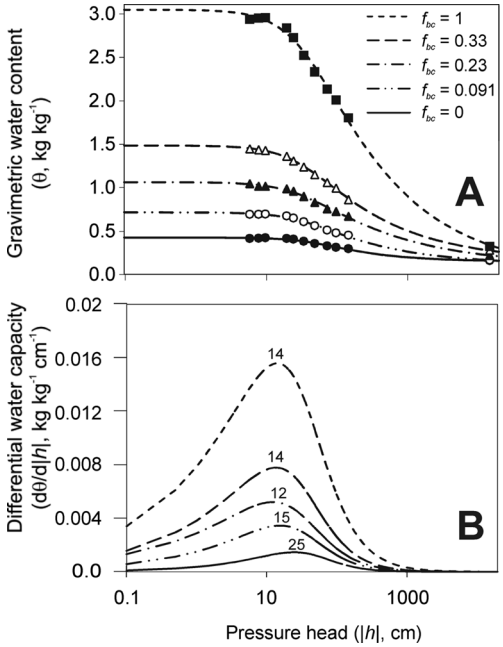

Fig. 1 **a** Fitting of the HEMC data by the van Genuchten Eq. (3). The points refer to the experimental pairs reported in Table 1. **b** Differential water capacity curves obtained for the different biochar fractions

water molecules distributed in the pore system of our study. The maximum of each distribution is the modal value which is inversely related to the most common pore size diameters present in each sample (Hillel 2004). The smaller the modal value, the larger is the pore diameter. Conversely, as the modal value increases, the pore diameter becomes smaller. Evaluation of the distributions in Fig. 1b evidences that the modal value decreases upon addition of progressive amounts of biochar to the sandy-clay soil up to f_{bc}=0.33. For f_{bc} values of 0.33 and 1, the modal value remained constant (Fig. 1b). These results not only confirmed that pore size diameters increased by biochar amendments but also revealed that by varying f_{bc} from 0.33 to 1 (i.e. sole biochar), no modal pore size increment was appreciated.

The van Genuchten retention function given in Eq. (3) was applied to fit the data points in Fig. 1a and to retrieve the van Genutchen parameters reported in Table 2 by applying the RETC code (see "Materials and methods").

The saturated water content (θ_s), which is related to the soil porosity, increased from 0.423 to 3.039 kg kg^{-1} (Table 2), thereby confirming the enhancement of the pore spaces available for water retention. Table 2 also shows no clear trend for the residual water content (θ_r) which is related to the amount of hygroscopic water. However, Fig. 2a evidences a progressive enhancement of the volume of drainable pores given by $\Delta\theta_g=\theta_s-\theta_r$, thereby suggesting that $\Delta\theta_g$ is only affected by θ_s values. As expected by the pore size enlargement reported above, both field capacity (θ_{fc}) and maximum available water ($\theta_{fc}-\theta_r$) also increase with the amount of biochar amendments (Fig. 2a).

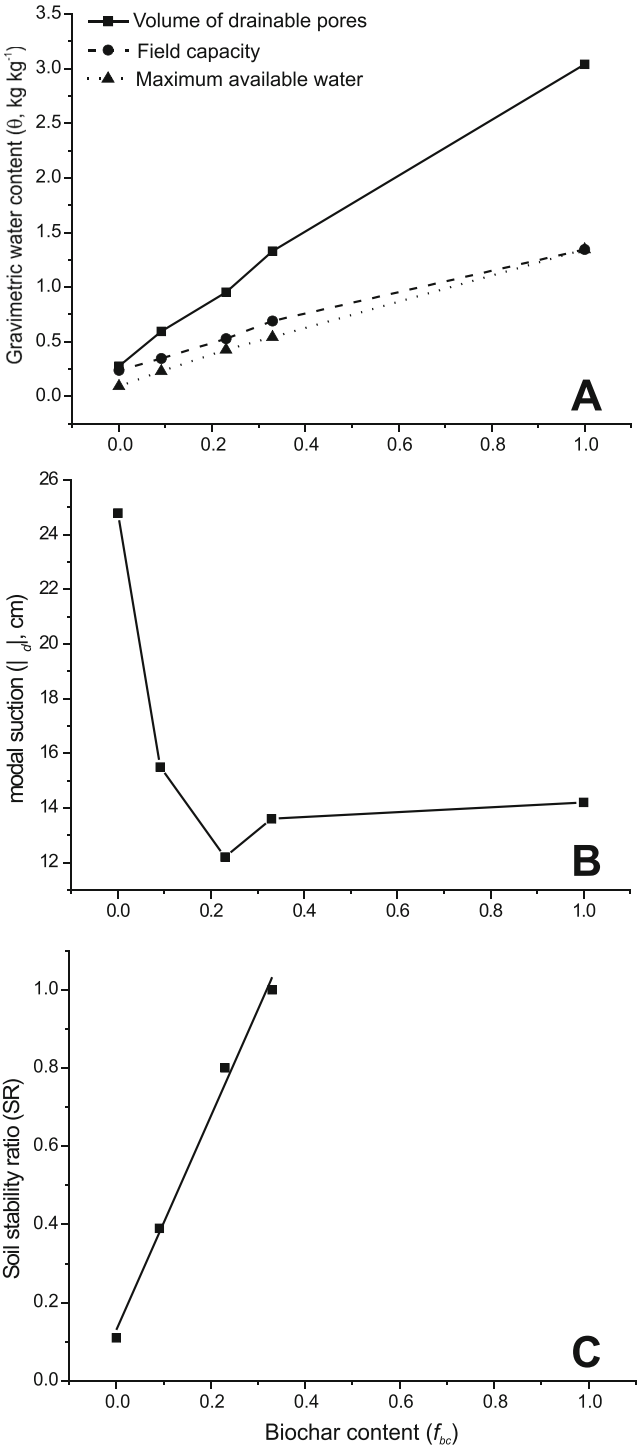

Fig. 2 **a** Gravimetric water content, **b** modal suction |τd| and **c** soil stability ratio (SR) dependence on biochar content (f_{bc})

The fitting of the van Genutchen equation to the experimental HEMC data (Fig. 1a) also provided the values for the shape parameters α, n and m (Table 2). α, related to the air entry potential, does not show any trend with f_{bc} variations. Conversely, both n and m (which are fitting parameters) slightly decreased with increasing f_{bc} values up to f_{bc}=0.33

(Table 2). For f_{bc}=0.33 and f_{bc}=1, n and m remained almost constant (Table 2). Application of the shape parameters in Eq. (5) resulted in the modal suction ($|\tau_d|$) values reported in Fig. 2b. Here, $|\tau_d|$ diminution was observed as f_{bc} ranged between 0 and 0.33, whereas no variations were observed for f_{bc}>0.33. The modal suction describes the water potential corresponding to the liquid constrained in the most common pore size diameters. For this reason, we may argue that the decrement of $|\tau_d|$ between f_{bc} 0 and 0.33 (Fig. 2b) is attributable to the pore enlargement as already outlined above. On the other hand, the constant $|\tau_d|$ values (Fig. 2b) together with the ΔU_g increment (Fig. 2a) for f_{bc}>0.33 allows to argue that as biochar content overcomes 33 % of the total system weight, the swelling processes predominate into the inter-aggregate porosity system.

Table 2 reports the *SR* values obtained for the different f_{bc} fractions, while Fig. 2c shows the linear trend for *SR* vs f_{bc}, thereby highlighting that aggregate stability increases by raising up the amount of biochar as a consequence of the cementing effect retrieved by the added organic material (Ouyang et al. 2013).

3.2 ^{1}H NMR relaxometry

Water molecular dynamics on the surface of a porous medium is related to pore size (Conte and Alonzo 2013). In fact, as water molecules flow through larger sized pores, their motion occurs at a frequency that is broader than that of water molecules constrained in smaller sized ones. Quickly moving water cannot efficaciously interact neither with the neighbouring molecules nor with the molecular sites on the surface at the liquid–solid interface. As a consequence, intermolecular dipolar interactions are weakened, and an increase of the proton longitudinal relaxation time (longer T_1 values) can be observed. On the contrary, as water systems are slowly moving or immobilized, as in smaller pores, dipolar interactions become stronger and T_1 values are shortened (Conte and Alonzo 2013). As the number and size of the various pores present in a material are heterogeneous, water must diffuse through the differently sized pores, thereby providing a wide ensemble of longitudinal relaxation times which appear continuously distributed. The lowest limit of such ensemble (the shortest T_1 value) is due to water moving into the smallest pores, whereas the highest limit (the longest T_1 value) is attributed to water moving into the largest spaces. All T_1 values between the two limits are due to the dynamics of water inside pores having sizes lying between the two extremes (Conte and Alonzo 2013).

It must be pointed out that water constriction is not only due to physical restrictions but also to chemical interactions with the functional groups on the surface of the porous media. As an example, water molecules on biochar surface can interact either with the inorganic ashes in biochar or with the biochar aromatic organic systems. In the first case, water-ash interactions are established through formation of charge-transfer bindings where the electrons, in the electron-rich oxygen present in water, fill the electron deficiencies in the metals belonging to ashes. Conversely, the interactions between water and the organic constituents of biochar can be obtained through the electron donation from the π-clouds of the polyaromatic systems towards the electron-deficient hydrogens in water, thereby leading to weak unconventional H bonds (Conte et al. 2013a). Similar weak H bonds have been also revealed between water and titanium dioxide polymorphs. In the latter case, the H bonds were established between oxygen in water and the hydrogens in the surface hydroxyls of TiO_2 (Conte et al. 2013b).

Figure 3 shows the proton longitudinal relaxation time distributions for the sandy-clay soil (f_{bc}=0), the soil added with biochar at three different weight fractions (f_{bc}=0.091, 0.23 and 0.33, respectively) and the sole biochar (f_{bc}=1).

The T_1 distribution of the sandy-clay soil shows only one symmetric band centred at 3 ms, whereas biochar reveals a wider T_1 distribution with the main maximum centred at 318 ms. The three sandy-clay soil/biochar samples uncover clear bimodal T_1 distributions with two maxima at around 4 and 92 ms. In particular, the intensity of the first broad band at around 4 ms lowers while that at around 92 ms raises up as the amount of biochar is increased (Fig. 3). It must be pointed out that the bimodal T_1 distribution did not correspond to a bimodal behaviour in the water capacity curve $d\theta/dh$. This is probably due to the fact that pressure head values, $|h|$, in the range 0–6 cm were not measured.

According to the mechanisms outlined above, the shortest T_1 value in the sandy-clay soil is attributable to water restrictions due to either physical or chemical motion inhibitions. Physical inhibition can be due to the clay content of the soil which traps water in small spaces, thereby preventing water

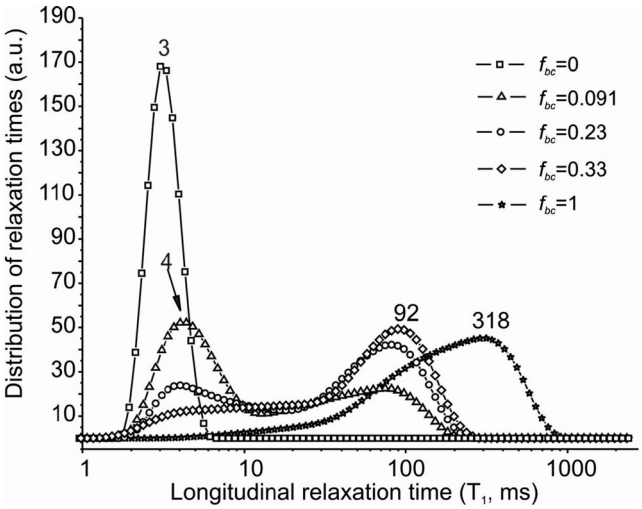

Fig. 3 T_1 distributions of the soil (f_{bc}=0), the biochar (f_{bc}=1) and the mixtures soil+biochar with f_{bc}=0.091, 0.23 and 0.33

free movements. Chemical inhibition is ascribable to formation of weak H bonds which chemically hook water to the surface functional groups of the sandy-clay soil. However, T_1 values are also dependent on the presence of paramagnetic impurities (e.g. Fe(III), Cu(II), Mn(VI), etc.) (Conte and Alonzo 2013) which were not measured in the present study. In fact, the magnetic moments and the local dipolar fields generated by the unpaired electron spins in the paramagnetic centres shorten the longitudinal relaxation time values of the proton spins in the diffusing water (De Pasquale et al. 2012).

The hydraulic properties of the sandy-clay soil (f_{bc}=0) have been discussed above. In particular, sandy-clay soil revealed the smallest volume of drainable pores (Fig. 2a), thereby indicating that the pore space available for water motion is very restricted. For this reason, we can rule out the effect of the paramagnetic centres on the relaxation mechanism of water in the sandy-clay soil and consider the physical and chemical motion inhibitions as predominant factors for proton spin relaxation.

The wideness of the T_1 biochar distribution (f_{bc}=1) (Fig. 3) can be explained by the larger pore size heterogeneity of such material as compared to the sole sandy-clay soil. In fact, the clayey nature of the soil makes it very compact and homogeneous in porosity (White 2006), thereby allowing reduction of the amount of large pore spaces and restricting water movements into and through the soil (see above). Conversely, biochar is a carbon-based material characterized by a very high and heterogeneous porosity (Pusceddu et al. 2013) which allows a better water drainage than the soil used in the present study (see results above).

The maximum at 318 ms and the shoulder at around 92 ms in the relaxogram of biochar reported in Fig. 3 indicate that water motion on biochar surface is faster than in sole soil because of the larger pore volume spanned by water. In fact, the larger the pore sizes, the longer is the time needed for nuclear relaxation (see above). This finding accords to the highest value of the drainable pore volume reported in Fig. 2a.

As biochar is increasingly added to the sandy-clay soil, the arrangement of the solid parts of the resulting mixtures and the dimension of the pore spaces located between them (i.e. the soil structure) change. As outlined in the previous paragraph, structure improvements with progressive biochar addition are due to the gluing effect of the organic material. Structure amelioration results in the enhancement of the drainable pore volumes, field capacity, maximum available water and soil structural index in the order: (f_{bc}=0)<(f_{bc}=0.091)<(f_{bc}=0.23)<(f_{bc}=0.33)<(f_{bc}=1) (Fig. 2a, c). A different order, (f_{bc}=0)>(f_{bc}=0.091)>(f_{bc}=0.23)≈(f_{bc}=0.33)≈(f_{bc}=1), is observed for the modal suction values (Fig. 2b).

Soil structural changes are evidenced by the bimodal distributions reported in Fig. 3. The latter are indications that water molecules are distributed in two different motion fractions. The fast relaxing fraction (band centred at around 4 ms) is generated by the water strongly bound into the intra-aggregate porosity system on to the surface of the sandy-clay/biochar mixtures. Conversely, the slow relaxing fraction (band centred at around 92 ms) is generated by the proton spin relaxation of less constrained water molecules in larger voids (i.e. the inter-aggregate porosity system).

It is worth of note that the relaxation bands of the three mixtures are displaced at different T_1 values as compared to those revealed for the sandy-clay soil (f_{bc}=0) and the sole biochar (f_{bc}=1) (Fig. 3). According to Lehmann et al. (2007) and Wagner et al. (2007), the mechanism for soil structure formation starts with the binding of the organic matter to the surface of the clay particles, thereby leading to formation of micro-aggregates. Afterwards, macro-aggregates are formed as a consequence of the micro-aggregate sandwiching. The random distribution of micro- and macro-aggregates into the soil/biochar mixtures explains the redistribution of pore sizes which is evidenced by the T_1 shifts reported in Fig. 3. Figure 3 also shows that the amount of slow moving water (band at 4 ms) decreases while the amount of fast moving water (band at around 92 ms) increases. This behaviour indicates that the amount of water spanning larger volumes and moving progressively faster increases, thereby according to the improvement of the volume of drainable pores reported in Fig. 2a.

4 Conclusions

This study aimed at the investigation of the effect of different amounts of biochar (f_{bc}) on the structure of a sandy-clay soil. Namely, the HEMC technique revealed that progressive additions of biochar increased soil aggregate stability by enhancing the volume of drainable pores, the field capacity, the maximum available water and the stability ratio. As a consequence of soil structure enhancement, a decrement of modal suction was measured up to an amount concentration biochar corresponding to f_{bc}=0.33. As f_{bc}=1, no variation in the modal suction was observed.

Modal suction measures the energy needed to remove water trapped in the pores having the most common diameter size. For this reason, the larger the pore diameter, the lower is the energy required for water to flow out from the pores. As the amount of biochar changed in the f_{bc} range 0–0.33, the modal suction reduction was associated to the enlargement of the volume of drainable pores, to the increasing of the field capacity and the maximum available water thereby indicating that intra-aggregate porosity was mainly involved in water retention. Conversely, as f_{bc} became larger than 0.33, the modal suction did not change while all the other parameters still increased. This behaviour was explained by considering that for f_{bc}=0.33, the inter-aggregate porosity was mainly involved in water retention through swelling processes.

The ^{1}H NMR relaxometry experiments revealed that water was tightly bound to the sole soil rather than to the sole biochar as a consequence of the wider size inhomogeneity of surface pores of the latter as compared to the former. As biochar was progressively added to the sandy-clay soil, a bimodal ^{1}H NMR relaxometry distribution was observed (i.e. two different longitudinal relaxation times, T_1, bands were detected). When water is tightly bound to the smallest sized pores, the shortest T_1 values are retrieved. On the other hand, water trapped in the largest pores need longer relaxation times due to weaker interactions with the solid phase surface. For this reason, the longest T_1 values are obtained.

It is worth noting that the intensity of the T_1 band associated to the loosely bound water increases while that of the tightly bound one decreases as f_{bc} is raised up. This behaviour has been attributed to the progressive enlargement of the volume of drainable pores as a consequence of biochar amendments. In fact, the amount of water molecules that are moving progressively faster increases as enlargement of pore diameter occurs.

This study not only confirmed the inter- and intra-aggregate dual soil porosity as reported in Alaoui et al. (2011) but also revealed that intra-aggregate porosity increased by biochar addition for f_{bc} ranging between 0 and 0.33. Conversely, inter-aggregate porosity resulted predominantly enhanced, through swelling processes, when f_{bc}>0.33. Further studies are needed in order to confirm the validity of the dual molecular water retention mechanisms upon biochar amendment by using different textured soils and chemically different biochars.

References

Agnese C, Baiamonte G, Corrao C (2001) A simple model of hillslope response for overland flow generation. Hydrol Process 15:3225–3238

Agnese C, Baiamonte G, Corrao C (2007) Overland flow generation on hillslopes of complex topography: analytical solutions. Hydrol Process 21:1308–1317

Agnese C, Bagarello V, Baiamonte G, Iovino M (2011) Comparing physical quality of forest and pasture soils in a sicilian watershed. Soil Sci Soc Am J 75:1958–1970

Alaoui A, Lipiec J, Gerke HH (2011) A review of the changes in the soil pore system due to soil deformation: a hydrodynamic perspective. Soil Till Res 115–116:1–15

Atkinson CJ, Fitzgerald JD, Hipps NA (2010) Potential mechanisms for achieving agricultural benefits from biochar application to temperate soils: a review. Plant Soil 337:1–18

Bagarello V, Baiamonte G, Castellini M, Di Prima S, Iovino M (2013) A comparison between the single ring pressure infiltrometer and simplified falling head techniques. Hydrol Process. doi:10.1002/hyp.9980

Chan KY, Van Zwieten L, Meszaros I, Downie A, Joseph S (2007) Agronomic values of green waste biochar as a soil amendment. Aust J Soil Res 45:629–634

Chan KY, Van Zwieten L, Meszaros I, Downie A, Joseph S (2008) Using poultry litter biochars as soil amendments. Soil Res 46:437–444

Collis-George N, Figueroa BS (1984) The use of soil moisture characteristics to assess soil stability. Aust J Soil Res 22:349–356

Conte P, Alonzo G (2013) Environmental NMR: fast-field-cycling relaxometry. eMagRes 2:389–398

Conte P, Marsala V, De Pasquale C, Bubici S, Valagussa M, Pozzi A, Alonzo G (2013a) Nature of water-biochar interface interactions. GCB Bioenergy 5(2):116–121

Conte P, Loddo V, De Pasquale C, Marsala V, Alonzo G, Palmisano L (2013b) Nature of interactions at the interface of two water-saturated commercial TiO_2 polymorphs. J Phys Chem C 117:5269–5273

Crescimanno G, Baiamonte G (1999) Hydraulic characterization of swelling/shrinking soils by a combination of laboratory and optimization techniques. In: Int. Workshop European-Society-of-Agricultural-Engineers, Field of Interest on Soil and Water on "Modelling of transport processes in soils at various scale in time and space", Leuven, Belgium, 24–26 November 1999

Crescimanno G, Iovino M, Provenzano G (1995) Influence of salinity and sodicity on soil structural and hydraulic characteristic. Soil Sci Soc Am J 59(6):1701–1708

Day D, Evans RJ, Lee JW, Reicosky D (2005) Economical CO_2, SO_x, and NO_x capture from fossil-fuel utilization with combined renewable hydrogen production and large-scale carbon sequestration. Energy 30:2558–2579

De Pasquale C, Marsala V, Berns AE, Valagussa M, Pozzi A, Alonzo G, Conte P (2012) Fast field cycling NMR relaxometry characterization of biochars obtained from an industrial thermochemical process. J Soils Sediments 12(8):1211–1221

Edwards AP, Bremner JM (1967) Microaggregates in soils. J Soil Sci 18: 64–73

Eswaran H, Rice T, Ahrens R, Stewart BA (2002) Soil classification—a global desk reference. CRC Press Boca Radon FL (USA)

Hillel D (2004) Introduction to environmental soil physics. Elsevier Science, London UK

Karhu K, Mattila T, Bergström I, Regina K (2011) Biochar addition to agricultural soil increased CH_4 uptake and water holding capacity—results from a short-term pilot field study. Agr Ecosyst Environ 140: 309–313

Kishimoto S, Sugiura G (1985) Charcoal as a soil conditioner. Int Achieve Future 5:12–23

Lehmann J, da Silva Jr JP, Steiner C, Nehls T, Zech W, Glaser B (2003) Nutrient availability and leaching in an archaeological Anthrosol and Ferralsol of the Central Amazon basin: fertilizer, manure and charcoal amendments. Plant Soil 249:343–357

Lehmann J, Kinyangi J, Solomon D (2007) Organic matter stabilization in soil microaggregates: implications from spatial heterogeneity of organic carbon contents and forms. Biogeochemistry 85:45–57

Levy GJ, Mamedov AI (2002) High energy moisture characteristic aggregate stability as a predictor for seal formation. Soil Sci Soc Am J 66:1603–1609

Li X, Zhang LM (2009) Characterization of the dual-structure pore-size distribution of soil. Can Geothec J 46:129–141

Liang B, Lehmann J, Solomon D, Kinyangi J, Grossman J, O'Neill B, Skjemstad JO, Thies J, Luizao FJ, Petersen J, Neves EG (2006) Black carbon increases cation exchange capacity in soils. Soil Sci Soc Am J 70:1719–1730

Mamedov AI, Wagner LE, Huang C, Norton LD, Levy GJ (2010) Polyacrylamide effects on aggregate and structure stability of soils with different clay mineralogy. Soil Sci Soc Am J 74: 1720–1732

Mikan CJ, Abrams MD (1995) Altered forest composition and soil properties of historic charcoal hearths in southeastern Pennsylvania. Can J Forest Res 25:687–696

Mualem Y (1976) A new model for predicting the hydraulic conductivity of unsaturated porous media. Water Resour Res 12:513–522

Ouyang L, Wang F, Tang J, Yu L, Zhang R (2013) Effects of biochar amendment on soil aggregates and hydraulic properties. J Soil Sci Plant Nutr 13(4):991–1002

Pierson FB, Mulla DJ (1989) An improved method for measuring aggregate stability of a weakly aggregated loessial soil. Soil Sci Soc Am J 53:1825–1831

Pusceddu E, Criscuoli I, Miglietta F (2013) Morphological investigation and physical characterization of ancient fragments of pyrogenic carbon. J Phys: Conf Ser 470:012003

Rawls WJ, Pachepsky YA, Ritchie JC, Sobecki TM, Bloodworth H (2003) Effect of soil organic carbon on soil water retention. Geoderma 116:61–76

Rillig MC, Wagner M, Salem M, Antunes PM, George C, Ramke HG, Titirici MM, Antonietti M (2010) Material derived from hydrothermal carbonization: effects on plant growth and arbuscular mycorrhiza. Appl Soil Ecol 45(3):238–242

Rondon MA, Lehmann J, Ramirez J, Hurtado M (2007) Biological nitrogen fixation by common beans (*Phaseolus vulgaris* L.) increases with bio-char additions. Biol Fert Soils 43:699–708

Sohi SP, Krull E, Lopez-Capel E, Bol R (2010) A review of biochar and its use and function in soil. Adv Agron 105:47–82

Spokas KA, Koskinen WC, Baker JM, Reicosky DC (2009) Impacts of woodchip biochar additions on greenhouse gas production and sorption/degradation of two herbicides in a Minnesota soil. Chemosphere 77:574–581

Stolte J, Veerman G (1991) Manual of soil physical measurements. Version 2.0 Winand Staring Centre (ed) Wageningen, the Netherlands

Uchimiya M, Lima IM, Klasson KT, Chang S, Wartelle LH, Rodgers JE (2010) Immobilization of heavy metal ions (CuII, CdII, NiII, and PbII) by broiler litter-derived biochars in water and soil. J Agr Food Chem 58:5538–5544

van Genuchten MT (1980) A closed-form equation for predicting the hydraulic conductivity of unsaturated soils. Soil Sci Soc Am J 44: 892–898

van Genuchten MT, ThLeij FJ, Yates SR (1991) The RETC code for quantifying the hydraulic functions of unsaturated soils. U.S. Salinity Laboratory, U.S. Department of Agriculture, Agricultural Research Service, Riverside, California

Wagner S, Cattle SR, Scholten T (2007) Soil-aggregate formation as influenced by clay content and organic-matter amendment. J Plant Nutr Soil Sci 170:173–180

Wallace J (2000) Increasing agricultural water use efficiency to meet future food production. Agr Ecosyst Environ 82(1–3):105–119

Warnock DD, Lehmann J, Kuyper TW, Rillig MC (2007) Mycorrhizal responses to biochar in soil—concepts and mechanisms. Plant Soil 300:9–20

White RE (2006) Principles and practice of soil science, 4th edn. Blackwell Publishing, MA, USA

Yuan JH, Xu RK, Wang N, Li JY (2011) Amendment of acid soils with crop residues and biochars. Pedosphere 21(3):302–308